



ELSEVIER

Resistivity anomalies in heavy-fermion CeCu_2Sb_2 and CeNi_2Sb_2

S.A.M. Mentink^{a,*}, B.J. van Rossum^a, G.J. Nieuwenhuys^a, J.A. Mydosh^a,
K.H.J. Buschow^b

^aKamerlingh Onnes Laboratory, Leiden University, 2300 RA Leiden, Netherlands

^bPhilips Research Laboratories, 5600 JA Eindhoven, Netherlands

Received 22 April 1994

Abstract

Temperature dependences of the electrical resistivity, magnetic susceptibility and specific heat of the tetragonal compounds CeCu_2Sb_2 and CeNi_2Sb_2 have been studied. The resistivity of both compounds displays a sharp maximum followed by a shallow minimum at higher temperature, indicative of heavy-fermion behavior. The possibility of anomalous low-energy crystalline electric field states is discussed by comparison with other cerium-based 1-2-2 compounds.

Keywords: Resistivity anomalies; Heavy fermions; Electrical resistivity; Magnetic susceptibility

1. Introduction

Anomalies in the temperature dependence of the resistivity, $\rho(T)$, and magnetic susceptibility, $\chi(T)$, are frequently observed in intermetallic compounds of Ce, Eu and Yb [1,2]. These anomalies originate from the unstable valence of the rare-earth component. In some cases a sharp maximum and subsequently a shallow minimum in $\rho(T)$ is observed. The series of tetragonal CeT_2X_2 -compounds (with T a transition metal and X a p-element) is particularly suited for a systematic study of such behavior [3]. With this contribution we extend this Ce-1-2-2 series by adding two new antimonides, CeCu_2Sb_2 and CeNi_2Sb_2 , and report their anomalous resistivity behavior. Our results are compared with those on the corresponding stannides CeCu_2Sn_2 and CeNi_2Sn_2 , and possible trends following from the different p-element constituents are discussed.

2. Metallurgical analysis and crystal structure

The samples of starting composition CeCu_2Sb_2 and CeNi_2Sb_2 were prepared by arc melting, using starting materials of at least 99.9% purity. After arc melting the samples were wrapped in Ta foil and annealed in evacuated silica tubes for 4 weeks at 800 °C. X-ray diffraction showed that the samples were almost single-

phase. The X-ray diagram could be indexed according to the tetragonal CaBe_2Ge_2 -type crystal structure. Possible site-disorder between the T-atom and Sb, however, cannot be excluded. The corresponding lattice constants, along with their Sn-based counterparts, are listed in Table 1.

Homogeneity and composition were investigated with electron probe microanalysis (EPMA). Our CeNi_2Sb_2 sample contains a grain-boundary phase (≈ 5 vol.%) of approximate composition Ni_9Sb_8 , with the relative composition of the grains being $\text{Ce}_{1.03}\text{Ni}_{2.02}\text{Sb}_{1.95}$. More interesting is the composition of our CeCu_2Sb_2 sample. EPMA clearly shows a considerable Cu deficiency, the actual composition being $\text{CeCu}_{1.3}\text{Sb}_2$. Such Cu deficiency is found in several 1-2-2 compounds with heavier p-elements, such as UCu_2Sn_2 [4], and should be contrasted with the excess amount of Cu needed to stabilize good

Table 1
Lattice constants, effective moments (μ_{eff}), Curie-Weiss temperatures (θ_{CW}) and temperature of the resistivity maximum (T_{max}) for CeT_2Sn_2 and CeT_2Sb_2 compounds

Compound	<i>a</i> (Å)	<i>c</i> (Å)	μ_{eff} (μ_{B}/Ce)	θ_{CW} (K)	T_{max} (K)	Ref.
$\text{CeCu}_{1.3}\text{Sb}_2$	4.341	10.256	2.51	-3.6	14.1	This work
CeNi_2Sb_2	4.416	9.967	2.40	-12.4	2.9	This work
CeCu_2Sn_2	4.433	10.355	2.49	-13.7	-	[11]
CeNi_2Sn_2 (<i>a</i> -axis)	4.437	10.126	2.61	-12.0	7.5	[15]

*Present address: Department of Physics, University of Toronto, 60 St. George Street, Toronto, Ontario, Canada.

superconducting samples of the heavy-fermion superconductor CeCu_2Si_2 [3]. The presence of some free Cu (approximately 5 vol.%) on the grain boundaries of $\text{CeCu}_{1.3}\text{Sb}_2$ will not influence the magnetic properties of the sample. Furthermore, the overall large resistivity (see below) of our CeCu_2Sb_2 sample indicates that no free-Cu conduction paths are formed, thus our results and the analysis of $\rho(T)$ are not affected. We will use the measured Ce–Cu–Sb composition to refer to this sample.

The electrical resistivity was measured in the range 0.35–300 K, using two different setups. For $T > 1.3$ K, a standard four-point d.c. technique was employed, while in our He-3 cryostat (0.35–4 K) we used an a.c. resistance bridge with a current of 0.3 mA operating at 16 Hz. No superconductivity was found down to 0.35 K. Magnetic measurements were performed using a Foner-type vibrating-sample magnetometer in the range $T = 1.6$ –300 K. The specific heat in zero magnetic field was measured from 1.8 to 40 K using an adiabatic heat-pulse method.

3. Results

The resistivity of $\text{CeCu}_{1.3}\text{Sb}_2$ is displayed in Fig. 1. Note that $\rho(T)$ is large over the entire temperature range. With decreasing T , the resistivity first decreases linearly down to $T_{\min} = 113$ K, before increasing strongly (suggesting the presence of a Kondo anomaly). A maximum is reached at $T_{\max} = 14.1$ K. At the lowest temperatures $\rho(T)$ decreases monotonously extrapolating to $\rho_0 = 108 \mu\Omega \text{ cm}$. The inset of Fig. 1 shows the temperature derivative of the resistivity, $d\rho(T)/dT$, which displays a distinct maximum at 3.5 K.

The results of the magnetic measurements for both samples are shown in Figs. 2 (solid line) and 3. Considering the $\text{CeCu}_{1.3}\text{Sb}_2$ compound first, Curie–Weiss behavior is observed for the susceptibility defined as

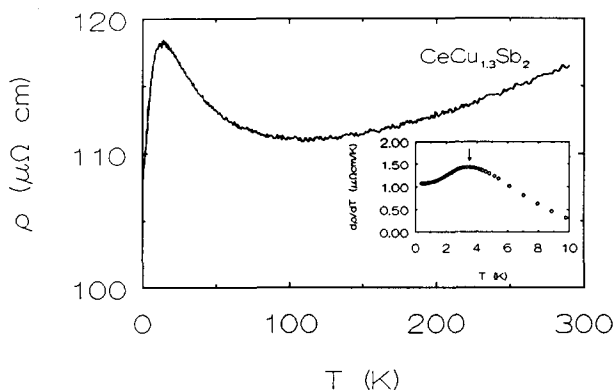


Fig. 1. Resistivity of $\text{CeCu}_{1.3}\text{Sb}_2$. The inset shows the temperature derivative below 10 K, which reaches a maximum at 3.5 K (indicated by the arrow).

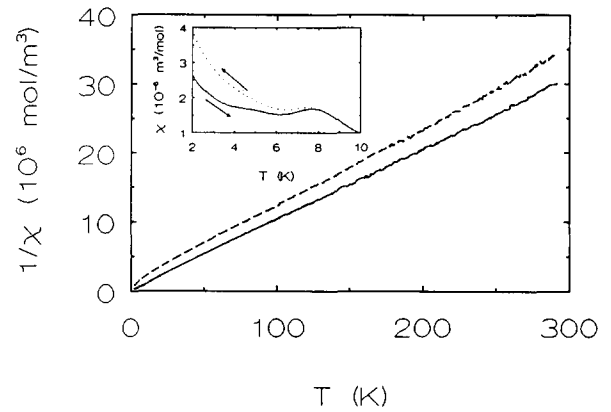


Fig. 2. Reciprocal susceptibility, $1/\chi(T)$, of $\text{CeCu}_{1.3}\text{Sb}_2$ (—) and CeNi_2Sb_2 (---). The inset shows $\chi(T)$ of $\text{CeCu}_{1.3}\text{Sb}_2$ below 10 K.

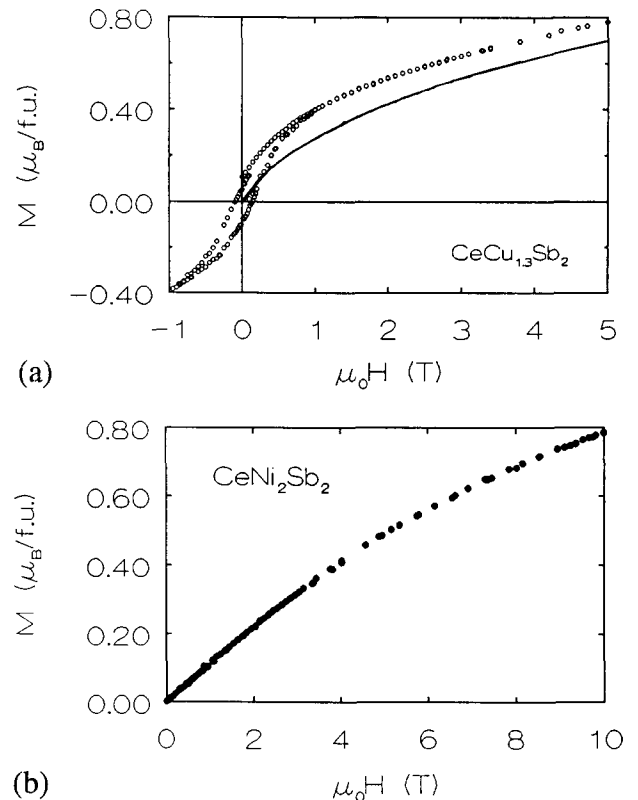


Fig. 3. Magnetization vs. field isotherms. (a) $\text{CeCu}_{1.3}\text{Sb}_2$ (—, $T = 4.1$ K, O, $T = 1.6$ K). (b) CeNi_2Sb_2 at $T = 4.3$ K.

the magnetization M divided by the magnetic field H , ($\chi = M/H$, measured in a field $\mu_0 H = 1.0$ T) over almost the entire temperature range, deviating only below 50 K. The effective moment and Curie–Weiss temperature derived from the high-temperature data equal $\mu_{\text{eff}} = 2.51 \mu_B/\text{Ce atom}$ and $\Theta_{\text{CW}} = -3.6$ K, respectively. The low- T susceptibility, $\chi(T)$, (measured in $\mu_0 H = 0.1$ T) of $\text{CeCu}_{1.3}\text{Sb}_2$ is displayed in the inset of Fig. 2. $\chi(T)$ reaches a maximum at $T = 7.7$ K, with considerable thermal hysteresis, indicative of complex magnetic order. Separate measurements of the magnetic isotherms at different temperatures suggest that a second type of

ordering does occur below approximately 4 K, related to the observed maximum in $d\rho(T)/dT$ at 3.5 K. As can be seen from the upper part of Fig. 3 ($\text{CeCu}_{1.3}\text{Sb}_2$), the magnetization is zero in zero applied field. A small metamagnetic-like transition is found in the 4.1 K isotherm, exhibiting a tiny hysteresis. This hysteresis is much more pronounced in the 1.6 K isotherm.

The specific heat of $\text{CeCu}_{1.3}\text{Sb}_2$ is shown in Fig. 4 (open circles). Again, the complexity of the magnetism is illustrated by two successive anomalies in c/T around 7.5 K (corresponding to the susceptibility maximum) and 4.4 K, respectively. We stress that no magnetic impurity phases or detectable amounts of cerium oxides are present in our sample, which implies that the observed anomalies are intrinsic properties of this compound. The inherent randomness of Cu-atom distribution over the available lattice sites can account for the smearing of the transitions, yielding the observed kinks in c/T (in accord with the values found for resistivity and susceptibility).

Our resistivity results on CeNi_2Sb_2 are shown in Fig. 5. While the overall behavior of $\rho(T)$ of this compound is similar to that of $\text{CeCu}_{1.3}\text{Sb}_2$, the characteristic temperatures are substantially lower than those of $\text{CeCu}_{1.3}\text{Sb}_2$. Here the minimum of $\rho(T)$ is located at $T_{\min} = 17.4$ K, while the maximum occurs at $T_{\max} = 2.9$ K. The T -dependence of the reciprocal susceptibility (measured in a field $\mu_0 H = 0.2$ T) is shown in Fig. 2 as the dashed line. The trend of $1/\chi$ is linear down to about 50 K, where a slight change of slope occurs. Above 50 K, the data obey the Curie–Weiss law with $\mu_{\text{eff}} = 2.40 \mu_B/\text{Ce}$ atom and $\Theta_{\text{CW}} = -12.4$ K. The magnetic isotherm at $T = 4.3$ K, displayed in the lower part of Fig. 3, has the general appearance of a paramagnet.

The specific heat of CeNi_2Sb_2 is displayed in Fig. 4 (closed circles). As the data above 20 K are equal to those of $\text{CeCu}_{1.3}\text{Sb}_2$, the phonon contribution to $c(T)$

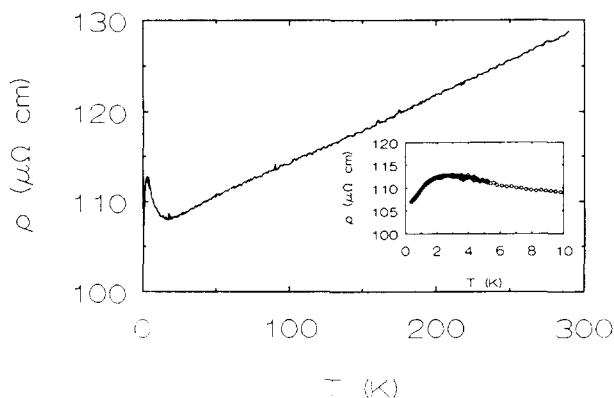


Fig. 4. Specific heat of $\text{CeCu}_{1.3}\text{Sb}_2$ (O) and CeNi_2Sb_2 (●), plotted as c/T vs. temperature. The rapid increase of c/T towards the lowest temperatures for CeNi_2Sb_2 is ascribed to a small CEF splitting of $\Delta_1 = 4.3$ K. The value of c/T of $\text{CeCu}_{1.3}\text{Sb}_2$ displays two anomalies at $T = 4.4$ and 7.5 K (see text).

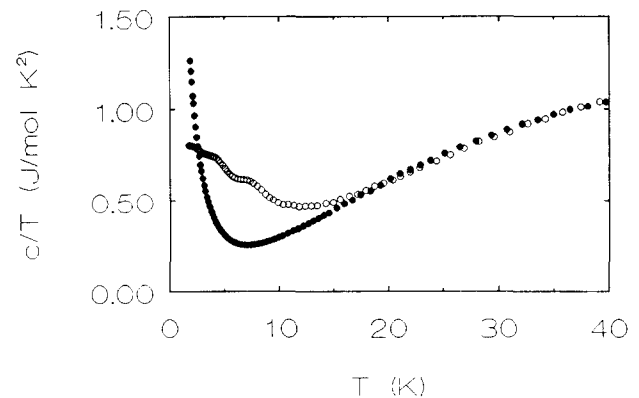


Fig. 5. Resistivity of CeNi_2Sb_2 down to 0.35 K. Inset shows the low-temperature maximum around $T_{\max} = 2.9$ K.

will be approximately the same for both compounds. Here, c/T increases rapidly below 7 K.

4. Discussion

We have prepared two novel Ce-based “1-2-2” compounds crystallizing in the tetragonal CaBe_2Ge_2 structure and studied their low- T properties. Both compounds show similar resistivity behavior, where the low-temperature maximum does not signal the onset of long-range magnetic order. For $\text{CeCu}_{1.3}\text{Sb}_2$ however, two successive magnetic transitions occur below 7.5 K and 4.4 K respectively, as evidenced by the susceptibility maximum, the kinks in the specific heat, the hysteretic magnetization and the distinct maximum in the temperature derivative of the resistivity. The magnetic-ordering temperature in these “1-2-2” compounds is mainly governed by the hybridization of the 4f-3d electrons of the cerium and transition metal ions [3,5]. As this hybridization strength becomes larger with decreasing Ce–T interatomic distance, the smaller c -axis value of CeNi_2Sb_2 and the larger T-atom content compared with $\text{CeCu}_{1.3}\text{Sb}_2$ will result in a decrease of the magnetic ordering temperature [6], in accord with the observed absence of magnetic ordering down to 0.35 K for CeNi_2Sb_2 .

The resistivity, susceptibility and specific heat of these compounds all characterize $\text{CeCu}_{1.3}\text{Sb}_2$ and CeNi_2Sb_2 as heavy-fermion systems. In this class of materials, $\rho(T)$ is strongly determined by the presence of a narrow 4f band close to the Fermi energy, the 4f states being strongly hybridized with 5d states and the 3d states of the transition metal ligands. The resistivity anomalies observed here may arise as a consequence of a strongly temperature-dependent quasiparticle lifetime of the 4f electrons [7,8], and the delicate balance between Kondo (T_K) and crystal-field (Δ_1 , the splitting between the two lowest doublets of the Ce^{3+} ion in tetragonal symmetry) energy scales [9,10]. The electronic specific-heat coef-

efficient γ for both $\text{CeCu}_{1.3}\text{Sb}_2$ and CeNi_2Sb_2 is estimated to be approximately $100 \text{ mJ mol}^{-1} \text{ K}^{-2}$. A definitive value will be determined by comparing with the non-magnetic La-based homologs.

We suggest that the ratio $T_K/\Delta_1 > 1$ in cerium-based 1-2-2 compounds with heavy p-elements or large c -axis values, i.e. for the CeT_2Sn_2 -series [11], CeCuAl_3 and CeCuGa_3 [12] and the CeT_2Sb_2 compounds presented here. This ratio should be contrasted with the $T_K/\Delta_1 < 1$ for most of the classical heavy-fermion compounds [13,14], where the crystalline electric field (CEF) splitting is of the order $\Delta_1 = 200 \text{ K}$, and the Kondo screening affects the ground-state doublet only. In the compounds investigated here, the Kondo effect acts on two low-lying doublets, which will be broadened and demagnetized. The CEF splitting has decreased considerably (evidenced by the absence of resistivity or susceptibility anomalies at around 100–200 K), and could become smaller than 20 K [15]. The depopulation of these levels with decreasing temperature may explain the (small) increase and subsequent decrease of $\rho(T)$, the deviations in $1/\chi$, and the specific heat anomalies at low temperatures (giving large c/T values). A rough estimate of the CEF splittings from our specific heat data yields $\Delta_1 = 4.3 \text{ K}$ for CeNi_2Sb_2 (accounting for the low- T upturn in c/T), consistent with the small decrease in the resistivity found below T_{max} . An estimate of Δ_1 for $\text{CeCu}_{1.3}\text{Sb}_2$ could not be made, owing to the magnetic ordering. Obviously, this approach is oversimplified, as all relevant contributions (Kondo effect, CEF splitting and magnetic interactions) have comparable energy scales and are therefore not separable.

A final remark concerns atomic site-order. Most noteworthy, a distribution of the transition metal and p-atoms over the sites available in the CaBe_2Ge_2 structure will randomize the magnetic interactions between the Ce-moments to some extent, as these interactions are mediated by the conduction electrons of the ligands. This atomic disorder could thus obscure possible long-range magnetic order, $\rho(T)$ being most sensitive (as

evidenced for CeCu_2Sn_2 [11]). In some cases, the definitive proof of long-range (anti-)ferromagnetism might only be established by neutron scattering. Such experiments and a more quantitative analysis of the resistivity data are planned in the near future.

Acknowledgments

This work is partially supported by the Dutch Foundation for Fundamental Research on Matter (FOM).

References

- [1] D.T. Androja and S.K. Malik, *J. Magn. Magn. Mater.*, **100** (1991) 126.
- [2] F. Steglich, *J. Magn. Magn. Mater.*, **100** (1991) 186.
- [3] F. Steglich, U. Ahlheim, C.D. Bredl, C. Geibel, M. Lang, A. Loidl and G. Sparn, in L.C. Gupta and M.S. Multani (eds.), *Frontiers in Solid State Sciences*, World Scientific Publishing Company, Singapore, to be published.
- [4] T. Endstra, personal communication.
- [5] T. Endstra et al., *Phys. Rev. B*, **48** (1993) 9595; *Ph.D. Thesis*, Leiden University, 1992.
- [6] S. Doniach, in R.D. Parks (ed.), *Valence Instabilities and Related Narrow-Band Phenomena*, Plenum, New York, 1977, p. 169.
- [7] M. Weger, *Philos. Mag. B*, **52** (1985) 701.
- [8] A. Freimuth, *J. Magn. Magn. Mater.*, **68** (1987) 28.
- [9] H.-U. Desgranges and J.W. Rasul, *Phys. Rev. B*, **32** (1985) 6100; *Phys. Rev. B*, **36** (1987) 328.
- [10] B. Cornut and B. Coqblin, *Phys. Rev.*, **5** (1972) 4541.
- [11] W.P. Beyermann, M.F. Hundley, P.C. Canfield, J.D. Thompson, M. Latroche, C. Godart, M. Selsane, Z. Fisk and J.L. Smith, *Phys. Rev. B*, **43** (1991) 13 130.
- [12] S.A.M. Mentink, N.M. Bos, B.J. van Rossum, G.J. Nieuwenhuys, J.A. Mydosh and K.H.J. Buschow, *Proc. 37th Annu. Conf. on Magnetism and Magnetic Materials, Houston, TX, 1992, J. Appl. Phys.*, **73** (1993) 6625.
- [13] A. Severing, E. Holland-Moritz, B.D. Rainford, S.R. Culverhouse and B. Frick, *Phys. Rev. B*, **39** (1989) 2557.
- [14] A. Loidl, K. Knorr, G. Knopp, A. Krimmel, R. Caspary, A. Böhm, G. Sparn, C. Geibel, F. Steglich and A.P. Murani, *Phys. Rev. B*, **46** (1992) 9341.
- [15] T. Takabatake, F. Teshima, H. Fujii, S. Nishigori, T. Suzuki, T. Fujita, Y. Yamaguchi and J. Sakurai, *J. Magn. Magn. Mater.*, **90&91** (1990) 474.